17th Australasian Fluid Mechanics Conference
Auckland, New Zealand
5-9 December 2010

Wind Turbine Wake Modelling using Large Eddy Simulation

S. E. Norris[1], J. E. Cater[2], K. A. Stol[1], and C. P. Unsworth[2]

[1]Department of Mechanical Engineering
[2]Department of Engineering Science
University of Auckland, Auckland 1142, New Zealand

Abstract

A Large Eddy Simulation (LES) code has been developed to simulate the atmospheric boundary layer passing through a wind farm. The wind turbines are modelled as actuator disks, and a simple model of a wind gust is implemented. The wake of a turbine is shown to extend downstream sufficiently far so as to affect downwind turbines.

Introduction

In recent years there has been an increasing interest in the use of wind turbines for electrical generation. For economic reasons the wind turbines are typically located close together in "wind farms", which almost inevitably leads to some turbines operating in the wake of their upwind counterparts [1]. A group at the University of Auckland is researching control strategies for wind turbines located within wind farms. To test the controllers the transient wind flowing through the farm is simulated using Large Eddy Simulation (LES), which allows the onset flow on the turbines to be affected by upstream events.

In this paper we discuss the techniques used for modelling the flow in an atmospheric boundary layer, in both the presence and absence of a wind turbine. The effect of a turbine's wake on a downstream turbine is discussed, and a simulation of a gust event passing through a turbine is presented.

To simplify the boundary conditions, the modelled farm is located on flat terrain or in the open ocean, and the wind turbine rotors are modelled using actuator disk theory.

The NORARM CFD Code

The simple geometry for the flow domain allows the use of a structured Cartesian mesh for the flow solver. The NORARM [2, 3] CFD code used is a transient finite volume code which employs an Adams-Bashforth based fractional step solver [4]. The code uses a colocated mesh with the advective terms being approximated using central differencing, and uses Rhie-Chow [5] interpolation to evaluate cell face mass fluxes. This results in a code that is second order accurate in both time and space. The equations are solved in a segregated manner and the fractional step solver negates the need for iterative coupling at each time step allowing for the efficient calculation of transient flows. The code is written in Fortran 95 and has been parallelised using both MPI and OpenMP allowing its use on both shared and distributed memory machines.

The subgrid scale turbulence is modelled with the standard Smagorinsky model [6] modified by the near wall damping model of Mason and Thomson [7]. The boundary conditions for the velocity at the ground are imposed using a rough wall function [8].

The modelling of the atmospheric boundary layer using LES demands appropriate inlet conditions to the flow domain. For an empty domain with no turbines the flow can be modelled as periodic in the stream-wise direction with the flow driven by an applied pressure gradient. For the flow around a wind turbine this is no longer suitable since the model will experience perturbations generated by its own wake. For this case the inlet flow is modelled as having a mean velocity profile given by the log law with perturbations to the mean flow being calculated using Mann's method [9]. A three dimensional box of turbulent fluctuations is simulated using a spectral scheme and at each time step a successive slice of this solution is used to perturb the inlet flow.

Alternatively, the inlet flow can be provided by using a flow field calculated for an empty domain using periodic boundary conditions which sweep through the data in a similar manner to that used in Mann's method.

The wind turbine rotor is modelled by an actuator disk, with the momentum loss of the flow moving through the turbine imposed via sinks in the momentum equations.

Modelling the Atmospheric Boundary Layer

A horizontally homogeneous pressure driven boundary layer was used for initial verification of the code. The flow through a $1440 \times 480 \times 600$ metre domain was calculated, with a target velocity of 18 m/s at 90 m height and a roughness height of $z_0 = 0.5$mm (calculated from Cook's formula for wind over open water [10]).

The domain used was periodic in the x and y directions, with a rough wall boundary condition imposed at the lower z boundary and a slip boundary condition (zero momentum flux) imposed on the upper z boundary. The flow was driven by a pressure difference imposed across the stream-wise (x axis) periodic boundaries. A $288 \times 96 \times 120$ cell mesh was used with a uniform cell spacing of 5 metres in the horizontal axes and an exponentially expanding distribution vertically.

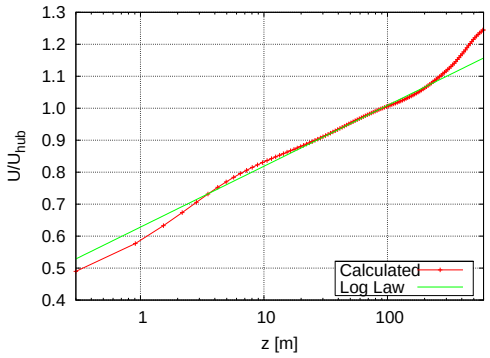

Figure 1: The mean velocity profile in the boundary layer compared with a logarithmic relationship.

The profile of the mean velocity in the developed boundary layer is shown in figure 1. This profile consists of three layers; below 10 metres; between 10 and 200 metres; and above

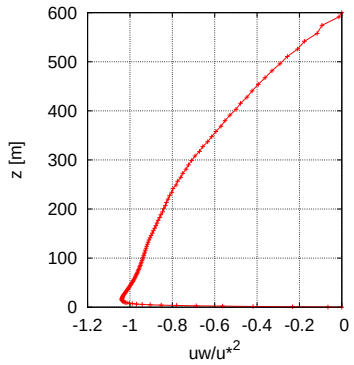

Figure 2: The profile of the mean *uw* Reynolds stress.

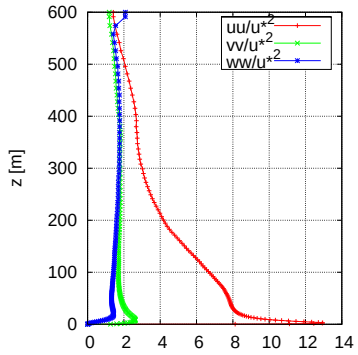

Figure 3: Profiles of the mean Reynolds stresses; *uu*, *vv* and *ww*.

200 metres. The region between 10 and 200 metres shows good agreement with the logarithmic layer prediction and this is the location in which the turbine operates. Below this height the velocity is less than the logarithmic profile. This suggests that the near wall damping function is insufficiently damping the eddy viscosity. Above 200 metres the velocity profile can be modelled by a logarithmic profile with a von Karman's constant that is lower than the generally accepted value of 0.4.

A logarithmic profile is not a good approximation for the flow as it is derived for a shear driven profile with a constant Reynolds stress across the layer. The flow currently modelled is pressure driven and has a Reynolds stress that decreases linearly from the lower boundary (shown in figure 2). The other significant turbulent stresses are shown in figure 3.

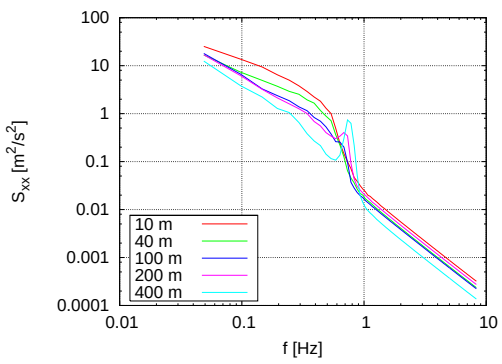

Figure 4: Power spectra of *u* velocity at 10 to 400 m elevation.

The power spectra at various elevations in the domain are shown in figure 4. The cutoff near 1 Hz corresponds to the limitations of the spatial resolution of the 5 m grid with a mean velocity of $\approx$ 20 m/s velocity field.

Modelling Turbines and their Wakes

The blades of the turbine are modelled using classical actuator disk theory [11]. The resistance provided by the turbine is based on an empirical thrust coefficient C_T,

$$F_T = C_T \frac{1}{2} \rho U_\infty^2 A \tag{1}$$

where A is the area of the disk, U_∞ the undisturbed velocity of the flow upwind of the turbine, and ρ is the density. For the LES model of the turbine located in a boundary layer U_∞ is no longer readily defined due to the turbulent fluctuations in the flow field, the effects of upwind turbines and the variation of the mean velocity with height. Instead, the methodology of [12] is used with the upwind velocity being calculated from the velocity at the turbine U_d and an assumed induction factor a,

$$U_\infty = \frac{U_d}{1-a}. \tag{2}$$

The turbine velocity U_d may be defined by taking a representative velocity (at the hub for instance), by averaging over the disk, or by using the local velocity in each finite volume.

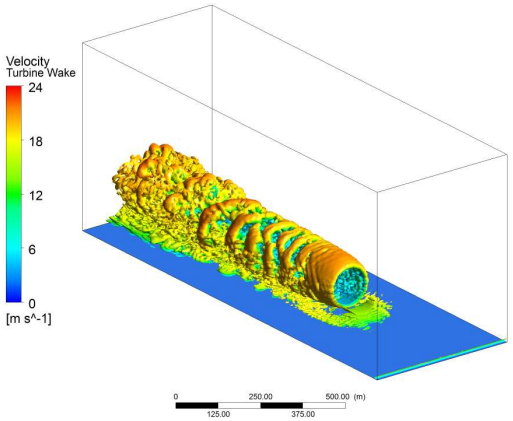

Figure 5: Instantaneous isosurfaces of velocity showing the wake of a single wind turbine.

The resistance due to the turbine is modelled as a momentum sink applied to the finite volumes intersected by the actuator disk. To ensure a smooth solution the disk is modelled as being two finite volumes thick and the force on each volume is

$$F_{FV} = \frac{C_T \rho U_d^2 A_{FV}}{4(1-a)^2} \tag{3}$$

with A_{FV} being the cross-sectional area of the actuator disk in the finite volume. The interpolation scheme for the cell face velocities is modified so that the momentum sink is interpolated separately from the velocities at the actuator disk, as done with the pressure field, preventing the creation of saw toothed velocity profiles.

The turbine model is based on the NREL 5-MW reference turbine [13] which has a hub height of 90 m and a rotor diameter of 126 m. Initial calculations have been made using values of

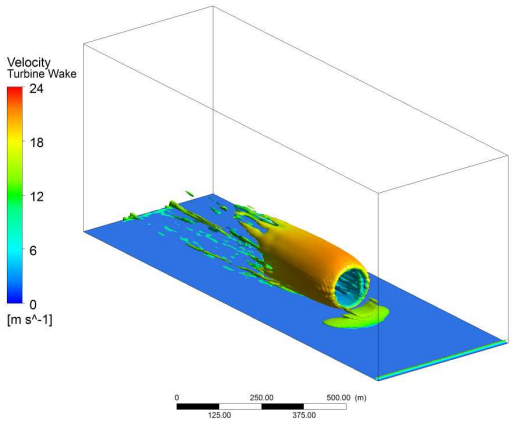

Figure 6: Time averaged velocity isosurfaces showing the wake of a wind turbine.

thrust coefficient and average induction factor from [12]. The values $C_T = 3/4$ and $a = 1/4$ are were used in this study.

The wake of the modelled turbine is shown in figures 5 and 6. The wake extends downwind and out of the calculation domain. The time averaged velocity along a line passing through the hub of the turbine is shown in figure 7, which shows how the velocity decreases through the turbine and for approximately $5D$ downwind before increasing again. This is significant since successive turbines may be located within $5-8D$ of each other [12].

The velocity profile in the wake $5D$ downwind of the turbine is shown in figure 8. Above 200 m the flow does not significantly differ from the upwind velocity profile. However, in the wake region at the hub height the velocity drops to approximately $1/5^{th}$ the upwind value.

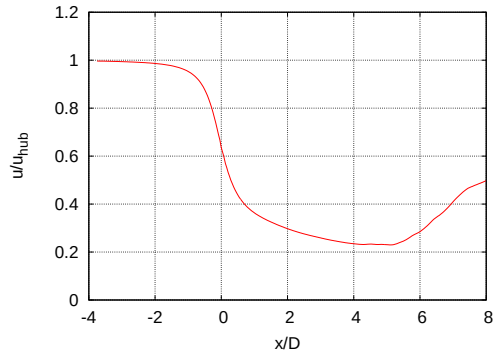

Figure 7: Time averaged velocity at the wind turbine hub height as a function of stream-wise distance in the domain. The turbine is located at $x/D = 0$.

Modelling a Gust

One of the control issues of interest is the case of an extreme gust passing through a wind farm. This can be modelled by having a prescribed inlet velocity profile on the upstream face of the computational domain. The inlet velocity varies in time to model a gust and the structure of the gust is convected downstream by the flow.

Whilst a definition of an extreme gust is provided by the British

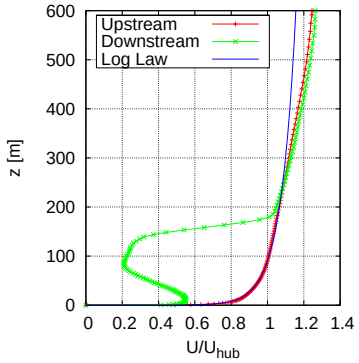

Figure 8: Profile of the time averaged velocity $4D$ upwind and $5D$ downwind of the wind turbine.

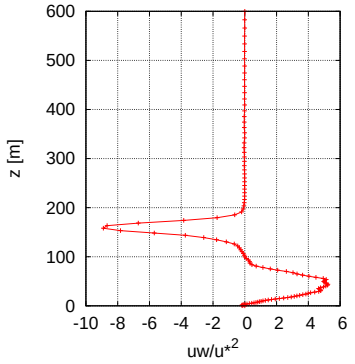

Figure 9: The profile of the mean uw Reynolds stress in the wake of the turbine. Profile $5D$ downwind of the turbine.

standard for wind turbine design [14], it is not useful for the LES model used here. The standard specifies a gust velocity profile as

$$u(z,t) = u_b(z) + u_g(t) \tag{4}$$

where $u_b(z)$ is the base velocity profile and $u_g(t)$ is given by

$$u_g(t) = \begin{cases} \frac{-U_g}{2.7}\sin\left(\frac{3\pi t}{T}\right)\left(1-\cos\left(\frac{2\pi t}{T}\right)\right) & : \quad 0 \le t \le T \\ 0 & : \quad \text{otherwise} \end{cases} \tag{5}$$

The gust lasts for a period T and uniformly perturbs the velocity profile through its entire vertical extent by a maximum of U_g. The standard specifies a gust period of 10.5 s (shown in figure 10). Whilst this may be of use when examining the flow passing through an isolated actuator disk, problems arise when modelling a boundary layer due to the incompressible nature of the flow and impermeable or periodic boundaries in the vertical and span-wise directions. A uniform increase in the velocity at the inlet as given in equation (4) leads to an instantaneous increase in velocity throughout the computational domain which is not physically representative of gust behaviour.

To prevent this, the gust perturbation must vary across the inlet and must integrate to zero so that the total mass flow through the inlet remains constant. A perturbation profile that has these properties is

$$u_g(z) = U_g \frac{z(1.2-0.36z/Z)}{Ze^{0.6z/Z}} \tag{6}$$

where Z is the height at which the gust is a maximum. Whilst (6) integrates to zero for an infinitely high domain, for regions of finite height it should be modified so that the integral equals zero exactly.

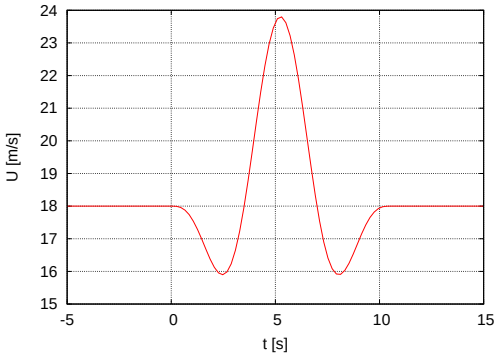

Figure 10: Variation of hub height velocity through a gust event, as prescribed by equation (5).

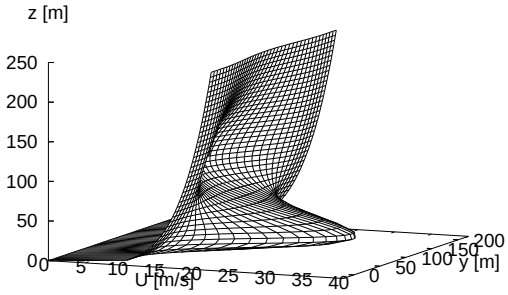

Figure 11: Gust velocity profile at $t = T/2$ given by (7)

.

Finally, the gust is given a width of Y and the resulting gust perturbation is

$$u_g(y,z,t) = U_g u_g(z) u_g(y) u_g(t) \quad (7)$$

$$u_g(y) = (1+\cos(2\pi y/Y))/2 \quad (8)$$

$$u_g(z) = \frac{z(1.2-0.36z/Z)}{Ze^{0.6z/Z}} \quad (9)$$

subject to the bounds $-Y/2 \leq y \leq Y/2$ with $u_g(t)$ being given in (5), the resulting velocity profile at $t = T/2$ being shown in figure 11.

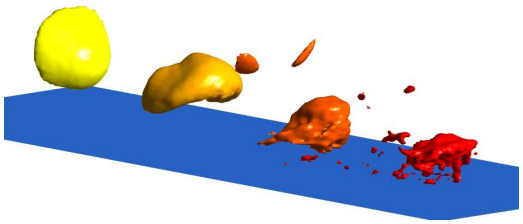

Figure 12: Four isosurfaces of velocity magnitude for a gust passing through the computational domain from left to right. The isosurfaces are evaluated at 15 second intervals from the start of the gust event; Yellow=15s, Red=60s.

A visualisation of a gust event is shown in figure 12. The region of fast moving flow is sheared by the boundary layer, breaks up and is dissipated by the modelled turbulence.

Conclusions

This work demonstrates the transient simulation of flow through a wind turbine located in the turbulent atmospheric boundary layer. An extreme wind event in the form of a model gust has been simulated and is shown propagating through the computational domain. Particular care must be taken when implementing gusts of this form due to computational mass flow constraints.

Acknowledgements

The authors acknowledge the support of the Faculty of Engineering at the University of Auckland through Faculty Research Development Funding.

References

[1] Hau, E., *Wind Turbines: Fundamentals, Technologies, Application, Economics*, Springer, 2006.

[2] Armfield, S.W., Norris, S.E., Morgan, P. and Street, R., A Parallel Non-Staggered Navier-Stokes Solver Implemented on a Workstation Cluster, in *Computational Fluid Dynamics 2002: ICCFD2*, editors S. Armfield, P. Morgan and K. Srinivas, 2003,30–45 .

[3] Norris, S., *A Parallel Navier–Stokes Solver for Natural Convection and Free Surface Flow*, PhD Thesis, University of Sydney, 2000.

[4] Armfield, S.W. and Street, R., An analysis and comparison of the time accuracy of fractional-step methods for the Navier-Stokes equations on staggered grids *I. J. Num. Meth. Fluids*, **38**, 2002, 255–282.

[5] Rhie, C.M. and Chow, W.L., Numerical Study of the Turbulent Flow Past an Airfoil with Trailing Edge Separation, *AIAA J.*, **21**, 1983, 1525–1532.

[6] Smagorinsky, J., General circulation experiments with the primitive equations. The basic experiment, *Mon. Weath. Rev.* **91**, 1963, 99–164.

[7] Mason, P.J. and Thomson, D.J., Stochastic backscatter in large-eddy simulations of boundary layers, *J. Fluid Mech.*, **242**, 1992, 51–78.

[8] Mason, P.J. and Callen, N.S., On the magnitude of the subgrid-scale eddy coefficient in large-eddy simulations of turbulent channel flow, *J. Fluid Mech.*, **162**, 1986, 439–462.

[9] Mann, J., Wind field simulation, *Prob. Engng. Mech.*, **13**, 1998, 269–282.

[10] Cook, N.J., *The designer's guide to wind loading of building structures* Butterworth-Heinemann, 1986.

[11] Betz, A., *Windenergie und ihre Ausnutzung durch Windmühlen*, Vandenhoek und Rupprecht, Göttingen, 1926.

[12] Calaf, M., Meneveau, C. and Meyers, J., Large eddy simulation study of fully developed wind-turbine array boundary layers, *Phys. Fluids*, **22**, 2010, 015110.

[13] Jonkman, J., Butterfield, S., Musial, W. and Scott, G., Definition of a 5-MW Reference Wind Turbine for Offshore System Development, *NREL/TP-500-38060*, 2009.

[14] Wind turbines. Design requirements *BS EN 61400-1:2005*, 2006.